# Supplementary Information

## Bacterial Elimination via Cell Membrane Penetration by Violet Phosphorene Peripheral Sub-Nanoneedles Combined with Oxidative Stress

Qiudi Shen,[a] Jing Kang,*[a] Xuewen Zhao,[b] Wanqing Lou,[c] Zhihao Li,[d] Lihui Zhang,[b] Bo Zhang,[b] Jinying Zhang, *[b] Bailiang Wang, *[c] Alideertu Dong*[a]

[a]*College of Chemistry and Chemical Engineering, Engineering Research Center of Dairy Quality and Safety Control Technology, Ministry of Education, Inner Mongolia University, 235 University West Street, Hohhot 010021, China*

[b]*State Key Laboratory of Electrical Insulation and Power Equipment, Center of Nanomaterials for Renewable Energy (CNRE), School of Electrical Engineering, Xi'an Jiaotong University, Xi'an 710049, China*

[c]*School of Ophthalmology & Optometry, Eye Hospital, Wenzhou Medical University, Wenzhou 325027, P. R. China*

[d]*Department of Chemistry, College of Sciences, Northeastern University, Shenyang 110819, China*

## Experimental Procedures

### 1. Materials

Violet phosphorus (VP) was supplied by the State Key Laboratory of Electrical Insulation and Power Equipment, Center of Nanomaterials for Renewable Energy, School of Electrical Engineering of Xi'an Jiaotong University. 4-Hydroxy-2,2,6,6-tetramethylpiperidinyloxy (TEMPOL) was purchased from Aladdin Biochemical Technology Co., Ltd. Sodium chloride (NaCl), sodium hydroxide (NaOH), ethanol absolute ($C_2H_6O$), and ethylenediaminetetraacetic acid ferric sodium salt (Fe (II)) were obtained from Tianjin Fengchuan Chemical Reagent Technologies Co., Ltd. Isopropanol alcohol (IPA) was purchased from Tianjin Fuyu Fine Chemical Co., Ltd. Sodium azide ($NaN_3$) was purchased from the Molecular Research Center, Inc. All chemicals were used without further purification. Microbiological culture media, including yeast extract powder and tryptone, were bought from Guangdong Huankai Biotech Co., Ltd. Beef cream was obtained from Beijing Aoboxing Biotech Co., Ltd. Agar was provided by Beijing Kulaibo Technology Co., Ltd. The microbial culture media were biological-reagent grade. Distilled water was used in all experiments and was generated by a Millipore system (Millipore Inc.). The live/dead cytotoxicity kit was purchased from Keygen Biotechnology Co. Ltd. (Nanjing).

### 2. Preparation of violet phosphorene nanosheets (VPNS) and black phosphorus nanosheets (BPNS)

Violet phosphorene nanosheets (VPNS) and black phosphorus nanosheets (BPNS) were synthesized via a convenient strategy based on a solvent exfoliation method. Typically, 80 mg of bulk violet phosphorus was prepared in advance by grinding it in a mortar, and then added it to 150 mL of ethanol absolute solvent. The suspension was ultrasonicated for 30 min using an ultrasonic cleaner at 200 W. Next, the suspension was ultrasonicated at 650 W and 98% power using an ultrasonic homogenizer (JY92-IIN Ningbo Xinzhi Biotech Co., Ltd) for 2 h under an ice bath. The obtained dispersion was centrifuged at 1,000 rpm for 10 min to remove the non-exfoliated bulk VP, then the supernatant was centrifuged at 15,000 rpm for 20 min to obtain ultrathin VPNS. After centrifugation, VPNS powder was obtained by triple washing with ultra-pure water and then vacuum freeze-drying.

### 3. Characterization of VPNS

The morphology and thickness of the VPNS were observed using a Hitachi SU8010 field emission scanning electron microscope (FESEM) at 5.0 kV, a Tecnai G2 20 transmission electron microscope (TEM), FEI Talos F200C TEM instrument (200 kV) equipped with an SC 1000 CCD camera (Gatan, Inc., USA), and a Brüker Dimension Icon atomic force microscope (AFM). Energy dispersive X-ray spectroscopy (EDS) line scanning and TEM mapping analyses were performed on a JEOL JEM-2100F high-resolution transmission electron microscope (HRTEM). The crystallinity of VPNS was investigated using a PANalytical Empyrean X-ray diffractometer (XRD). X-ray photoelectron spectra were obtained with an ESCALAB 250Xi XPS system (Thermo Fisher Scientific) and monochromated Al-Kα radiation (1486.6 eV, 150 W). The Raman spectra (Raman) of the VPNS were observed using a HORIBA Scientific LabRAM HR Evolution Raman spectrometer with an excitation laser wavelength of 514 nm at room temperature. The generation of reactive

oxygen species (ROS) in VPNS under different conditions was studied by electron spin resonance (ESR) spectroscopy on a JEOL JES FA200 spectrometer.

**4. Bacterial cell culture**

*Escherichia coli* (*E. coli*, ATCC 8099, a Gram-negative bacterium) and *Staphylococcus aureus* (*S. aureus*, ATCC 6538, a Gram-positive bacterium) were used as the two model strains in antibacterial tests. *Escherichia coli* pUC19 (*E. Coli* pUC19, a Gram-negative bacterium) and methicillin-resistant *Staphylococcus aureus* (MRSA, a Gram-positive bacterium) were used as two model resistant bacteria strains. Briefly, a single colony was inoculated under constant shaking at an average speed of 220 rpm in 5 mL of Luria-Bertani growth medium (LB) at 37 °C for 12 h, then the culture was allowed to expand to $10^8$–$10^9$ colony forming units (CFU) $mL^{-1}$.

**5. Antibacterial assay**

The antibacterial activity of VPNS was evaluated by the colony-counting method using *Escherichia coli* (*E. coli*, 8099 Gram-negative bacteria), *Staphylococcus aureus* (*S. aureus*, ATCC 6538 Gram-positive bacteria), methicillin-resistant *S. aureus*, and *E. coli* pUC19 as bacterial models. Generally, the bacterial strains were incubated in a shaker at a speed of 220 rpm for 12 h and a temperature of 37 °C to obtain bacterial strain concentrations of $10^8$–$10^9$ $CFU{\cdot}mL^{-1}$ for subsequent use. First, 1.0 mL of bacterial liquid with a concentration of $10^8$–$10^9$ $CFU{\cdot}mL^{-1}$ was absorbed and centrifuged at a speed of 4000 rpm for 7 min. Next, the liquid medium was poured out and the precipitated bacterial strains were washed three times with 0.9 wt% sodium chloride aqueous solution and then redispersed in 1.0 mL of sterile distilled water. The bacteria concentration was diluted to $10^7$ $CFU{\cdot}mL^{-1}$. 1.0 mg of VPNS was dispersed in 900 µL of sterile distilled water, and 100 µL of the above bacterial liquid was added and then put into a shaker for 3 h at room temperature. The mixture was diluted step by step to $10^2$ $CFU{\cdot}mL^{-1}$ and spread evenly on LB agar plates. The mixture was inverted in an incubator at 37 °C for 12 hours and 24 hours, respectively. In order to explore the influence of light conditions on antibacterial performance, the antibacterial operation of VPNS was carried out without light, in natural light, and under LED white light (5 W, PCX50C Discover, Beijing Perfect Light Technology Co., Ltd.). All experiments were repeated three times, and the antibacterial rate was calculated according to the following formula:

$$\text{Antibacterial rate } \% = (B-A) / B \times 100\ \%$$

where A is the number of surviving colonies for the sample and B is the number of surviving colonies for the control.

To explore the role of light in the antibacterial, the antimicrobial assays were carried out under different light conditions: in the dark, under natural light, and under LED white light, in which an LED lamp (5 W, PCX50C Discover, Beijing Perfect Light Technology Co.,Ltd.) was used as the white light source.

**6. Minimum Inhibitory Concentration (MIC) Assay**

Minimum inhibitory concentration (MIC) determination is to determine the lowest concentration of the antimicrobial substance that inhibits the growth of bacteria. Bacteria were cultured in LB medium for 12 h at 37°Cunder shaking at 220 rpm. Then the bacterial suspension was centrifuged at 4000 rpm for 7 minutes to collect bacterial cells. After being re-suspended in LB medium, the cells were diluted in LB medium to a cell density of $2\times10^6$ CFU $mL^{-1}$ as the working suspension. The VPNS were dispersed to concentrations ranging from 1.0 to 0.1 mg $mL^{-1}$ in a 96-well plate. After mixing equal volumes of bacterial cell suspension and VPNS solution, the 96-well plates were incubated at 37°C for 12 h. LB medium was used as the blank, the bacteria and LB medium mixture was used as the positive control in the same 96-well plate. The optical density (OD) value was collected by using a microplate reader. The percentage of bacterial growth was calculated according to the following formula:

Cell growth $\%=OD_{VPNS} - OD_{blank} / OD_{Control} - OD_{blank}\times100\%$

An aliquot of 1.0 μL bacterial suspension from each well of the above final mixture in the MIC study was transferred to an LB agar Petri dish. After incubating the plate at 37°C for 12 h, the MBC value was determined by visually checking the bacterial growth. This experiment was repeated at least twice after the repeats of the MIC test.

**7. Live/Dead BacLight bacterial viability kit testing**

After the bacterial samples were treated with VPNS, the viability and membrane integrity of *E. coli* were assessed using a Live/Dead BacLight staining kit. The kit utilized SYTO 9 and propidium iodide to quantify the killed bacteria and the viable bacteria through fluorescence microscopy photographs. Briefly, $1\times10^8$ CFU·$mL^{-1}$ *E. coli* and VPNS materials were inoculated for 3 h and irradiated under natural light. After sterilization, the VPNS and bacterial solution were separated by centrifugation, then the obtained bacterial solution was gathered by centrifugation at 4000 rpm, and the supernatant was poured out and added into 10 μL of sterile water to disperse the bacteria again. Next, 10 μL of the bacterial solution was mixed with 10 μL of the propidium iodide/SYTO 9 mixture and incubated at room temperature in the dark for 20 min. 10 μL of stained bacterial sample was trapped between a slide and a square coverslip. The fluorescence was examined using an inverted confocal fluorescence microscope (LSM710, Carl Zeiss Co., Ltd.).

**8. Scavenging study**

A scavenging experiment was carried out to determine whether four ROS species contribute to VPNS's bactericidal functionality under light irradiation. Four trapping agents were each added to 1.0 mg of VPNS sample: TEMPOL (0.6 Mm) for $\cdot O_2^-$, IPA (0.25Mm) for ·OH, Fe(II) (0.24 Mm) for $H_2O_2$, and $NaN_3$ (0.015 M) for $^1O_2$. The scavenging experiment was carried out under the same conditions as the above-described antibacterial test. Typically, 1.0 mL of bacterial liquid with a concentration of $10^7$ CFU·$mL^{-1}$ was added to the above mixture and incubated for 3 hours under light conditions. After incubation, the bacterial solution was diluted stepwise to $10^2$ CFU·$mL^{-1}$ and spread evenly on LB agar plates, then cultivated at 37 °C for 12 h. The colony counting experiment was carried out in parallel for the three groups to ensure the accuracy of the experiment. The

surviving colonies on each LB agar plate were counted, and the corresponding antibacterial rate was calculated.

**9. Bacterial morphology observations**

TEM and SEM were employed to observe the bacterial morphologies before and after treatment with VPNS. About 1.0 mg of VPNS sample was ultrasonically dispersed in 900 μL of aseptic distilled water. Then 100 μL of $1 \times 10^7$ CFU·mL$^{-1}$ bacterial solution (*E. coli* and *S. aureus*) was added to the suspension of the sample for 3 h under light conditions. The supernatant was poured out after centrifugation for 7 min at 4000 rpm. The bacterial cells were washed with sterilized PBS buffer three times, and the obtained bacterial cells were fixed overnight with 2.5% (w/v) glutaraldehyde at 4 °C. The as-obtained mixture was washed with PBS at least three times, and dehydrated with 20%, 50%, 80%, and 100% ethanol in turn. The mixture was then sat for 10 min and centrifuged for 7 min. Afterward, the mixture was washed twice with t-butanol and then dispersed in t-butanol. The resulting mixture was dripped separately onto copper net mesh and silicon wafer to observe its appearance. Finally, the morphology of the bacteria was observed by SEM and TEM.' has been described in the supporting information.

**10. DNA leakage test**

Take 1.0 mL of $10^8$ CFU ·mL$^{-1}$ bacterial suspension and wash it three times with PBS. Then, 9.0 mL VPNS solution with a concentration of 1.0 mg/mL was added, and incubated under LED light irradiation. 1.0 mL solution was extracted and filtered with 0.22 μm filter membrane every 30 minutes. The filtrate was then placed on a UV-vis spectrophotometer to measure the absorbance at 260 nm.

**11. Inhibition zone tes**t

About 1.0 mg of VPNS, BPNS, and $AgNO_3$ were each ultrasonically dispersed in 500 μL of deionized water, and all the obtained dispersions were uniformly dropped onto filter paper. Then *E. coli* in a concentration of $10^5$ CFU·mL$^{-1}$ was spread flat on the medium for drying, and the filter paper with the loaded sample was placed in the middle of the medium for 12 h at 37 °C. The antibacterial ability of the samples was evaluated by observing the size of the inhibition zones.

**12. CCK-8 assay**

All cells were purchased from National Collection of Authenticated Cell Cultures. Ethical permission for the cells experiment was obtained from Inner Mongolia University and Wenzhou Medical University. The cytotoxicity of the VPNS was evaluated by CCK-8 *in vitro* cytotoxicity analysis, with NIH 3T3 and Raw 264.7 cells as the cell model. Specifically, NIH 3T3 cells (7000 cells/well) and Raw 264.7 cells (7000 cells/well) were inoculated in a 96-well plate containing 180 μL and incubated at 37 °C for 24 h. The VPNS were dispersed with sterile PBS, and the samples were prepared at concentrations of 0.125, 0.25, 0.5, 1.0, and 2.0 mg·mL$^{-1}$. Next, 20 μL of the VPNS was added to each well of NIH 3T3 cells and Raw 264.7 cells cultured as described above, then incubated at 37 °C for 24 h. The cultured mixture was washed twice with PBS, into each well

was added 150 μL of the prepared 10% (V/V) CCK-8 solution, and the wells were incubated at 37 °C for 2 h. The OD value at 450 nm was measured with a microplate microscope.

**13. MTT assay**

The cytotoxicity of VPNS was evaluated using the 3-(4,5-dimethylthiazol-2-yl)-2,5-diphenyltetrazolium bromide (MTT) method. Briefly, $8.0 \times 10^3$ adherent L02 cells were inoculated in a 96-well plate containing 10% FBS in each well, then placed in a $CO_2$ incubator at 37°C, 5% $CO_2$, and 100% humidity. After incubation overnight, a series of VPNS samples in concentrations of 0.125–2.0 mg·mL$^{-1}$ were added to each well for incubation for 48 h. Then 20 μL (5 mg·mL$^{-1}$) of MTT was added and incubated at 37 °C for 4 h, followed by 150 μL of dimethyl sulfoxide (DMSO) to dissolve the purple crystals of formazan. Experimental data were obtained by measuring the absorbance at 492 nm on an HSB-1096A microplate in Nanjing, China.

**14. Live/dead staining**

Typically, $3.6 \times 10^5$ L02 cells and $5.4 \times 10^5$ HCEC were seeded in 6-well plates containing 2 mL of DMEM medium and 10% FBS for 24 h. The cells were then treated with a series of VPNS samples in concentrations of 0.125–2 mg·mL$^{-1}$ for 24 h, then washed with PBS buffer three times to remove the medium. The cells were then stained for 30 min using Live/Dead Viability/Cytotoxicity Kits. Finally, the cells washed with PBS buffer were observed under a IX71 fluorescence microscope (Olympus, Tokyo, Japan). Living cells were stained green by Calcein AM, and dead cells were stained red by EthD-1.

**15. TUNEL staining**

TUNEL staining was used to detect apoptosis and evaluate the cytotoxicity of the VPNS. Specifically, L02 cells (5000 cells/well) were inoculated in a 12-well plate containing 180 μL and incubated at 37 °C for 24 h. Next, the L02 cells were treated with a series of VPNS samples in concentrations of 0.125, 0.25, 0.5, 1.0, and 2.0 mg·mL$^{-1}$ for 24 h, then washed with PBS buffer three times. The cells were treated with DAPI (5 μg·mL$^{-1}$) and 50 μL of TUNEL, then incubated for 5 min. Finally, the L02 cells were washed with PBS buffer and observed using a IX71 fluorescence microscope (Olympus, Tokyo, Japan).

**16. Hemolysis test**

Fresh blood was harvested from BALB/c mice, then it was centrifuged at 1,500 rpm for 10 min in 1 × PBS (pH = 7.2) to remove broken red blood cells. An erythrocyte suspension was incubated with VPNS samples in different concentrations (2–0.0625 mg·mL$^{-1}$) at 37 °C for 3 h. Triton X-100 was used as the positive control, while PBS buffer was used as the negative control. After incubation, the VPNS sample was removed, and the erythrocyte stock solution was centrifuged at 1500 rpm for 10 min to obtain the supernatant. Then the absorbance of the supernatant was measured at 578 nm using the UV-vis spectrum (HITACHI U3900). The hemolysis rate was calculated by the following formula:

hemolysis (%) = $(A–A_{PBS}/A_0–A_{PBS}) \times 100\%$,

where A is the absorbance of the VPNS, $A_0$ is the absorbance of the positive control Triton X-100, and $A_{PBS}$ is the absorbance of the negative control PBS buffer

**17. Theoretical calculations**

The structures of black phosphorene and violet phosphorene were acquired from a crystal structure database. Two layers of violet phosphorus and four layers of black phosphorus were constructed. The size of the super cell was approximately 37×37×21 angstroms. Then two solvent layers were added to the upper side and the bottom, and a water–phosphorus interaction model was built. First, geometric optimization was carried out to remove improper overlaps in the models. Then molecular dynamic simulation of the NPT ensemble was employed to investigate the system changes under 1.0 atm of pressure in a 20 ns simulation. All simulations were finished with the Material Studio 2017 software package.

**18. *In vivo* wound treatment test**

Ethical permission for the mice experiment was obtained from the Animal Center of Inner Mongolia University. Wound healing in mice was used to evaluate the therapeutic effect of wound healing *in vivo*. Four-week-old BALB/C male mice were purchased from the Experimental Animal Center of Inner Mongolia University and fed in the animal laboratory for seven days to adapt them to the environment. The mice were anesthetized with an intraperitoneal injection of 10% chloral hydrate before the operation. The mice were divided into seven groups: healthy group, VPNS under light group, VP under light group, BPNS under light group, BPNS in the dark, light alone group, and control group. In all groups except the healthy group, a hole punch was used to make a 4 mm wound on the back of each mouse. The mice model of *Staphylococcus aureus* infection was used to evaluate the antibacterial activity *in vivo*. 10 μL of $10^8$ CFU·mL$^{-1}$ *S. aureus* bacterial liquid was injected into the wound. Then, samples of VPNS, VP, or BPNS were dropped on the wounds of the mice in the groups VPNS under light, VP under light, and BPNS under light, and light was shone for 3 h at room temperature. In the BPNS alone group, only BPNS was added to the wounds, without light. The samples were reapplied every day. Wound healing was observed each day by taking digital photographs and measuring the size of the wound area. The wound healing rate was calculated by the following formula:

Wound healing rate (%) = $(1-A_t/A_0) \times 100\%$

where $A_0$ is the initial wound area and $A_t$ is the wound area at a certain time interval.

After the wound had been treated with the sample for 7 days, blood from the mice's eyes was taken for routine blood tests. In addition, tissues at the wound site were collected. Grind the tissue with a grinder and disperse it in sodium chloride and incubated in LB agar plates at 37 °C for 24 h to observe the recovery of the infected wound, and the others were made into tissue sections to observe infection and inflammation.

**19. *In vivo* bacterial keratitis treatment**

Sprague Dawley (SD) rats about 150 g in weight were purchased from the Animal Administration Center of Wenzhou Medical University, randomly divided into five groups (5 rats per group). All

animals received care in compliance with the guidelines outlined in the Guide for the Care and Use of Laboratory Animals, and all animal experiments were approved by the Institutional Animal Care and Use Committee of Wenzhou Medical University. Firstly, SD rats were anesthetized by intraperitoneal injection of 10% chloral hydrate, Afterward, the rats were placed under a stereomicroscope (Optec SZ 680, China), and the corneal epithelium was scraped using a surgical knife. A 10 μL suspension of MRSA (~$1.0\times10^7$ CFU/mL) was placed on the corneal wound and incubated for 24 hours to successfully establish a bacterial keratitis animal model. After that, samples of PBS, VPNS, BPNS, and levofloxacin were dropped into corneas already infected with bacteria, where the light-stimulated treatment group was illuminated with LED lights for 3 hours. Corneal recovery was observed by slit-lamp and captured on day 0, 1, 3, 5, 7, and 9 after treatment, and clinical inflammation scores were performed according to Peyman's method. On day 9, the rats were euthanized and their corneas were removed for further histological evaluation and immunofluorescence staining.

**20. For H&E staining of corneas**

The cornea was first fixed for 2 h in a 4% paraformaldehyde solution at 4 °C, followed by dehydration with a series of sucrose solutions of different concentrations. Then, the tissues were immersed in optimal cutting temperature compound (O.C.T compound, Sakura, USA) at 4°C for 3 h, and sectioned at 10 μm on a freezing microtome (HM525, Thermo Fisher). Afterward, H&E staining was conducted on a Leica Autostainer XL (ST 500), and images of all sections were captured by a Leica DM4 B microscope.

**21. For inflammatory factor analysis**

For inflammatory factor analysis, the sections were incubated with primary antibodies against IL-1β, IL-6, and TNF-α overnight at 4 °C. Afterward, the sections were incubated with the secondary antibody (goat anti-rabbit lgG conjugated with Alex Fluor 594) at 37°C for 1 h. Finally, the sections were sealed by the antifade mounting medium with DAPI (P0131,Beyotime), and images of all sections were captured by a Leica DM4 B microscope.

## Results and Discussion

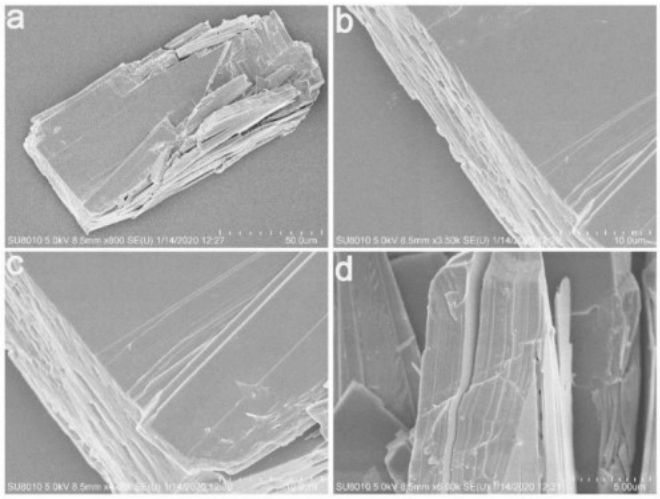


**Fig. S1.** SEM of bulk violet phosphorus, showing its multilayer structure.

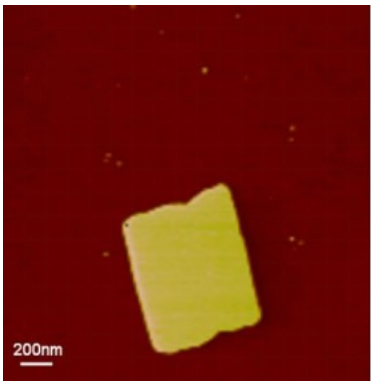


**Fig. S2.** AFM image of VPNS obtained from solvent exfoliation.

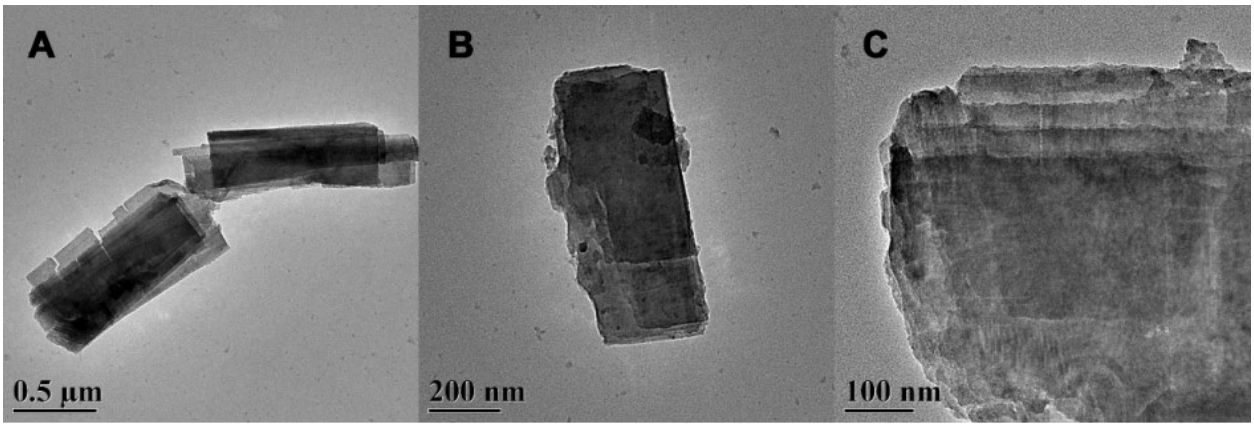


**Fig. S3.** TEM images of VPNS at different magnifications.

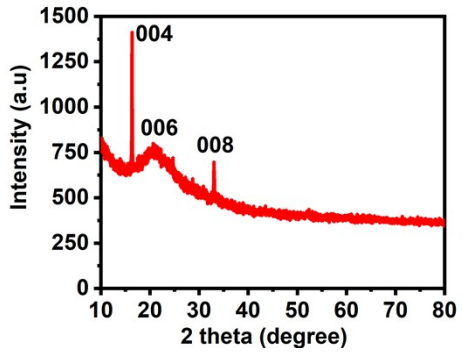


**Fig. S4.** XRD pattern of VPNS.

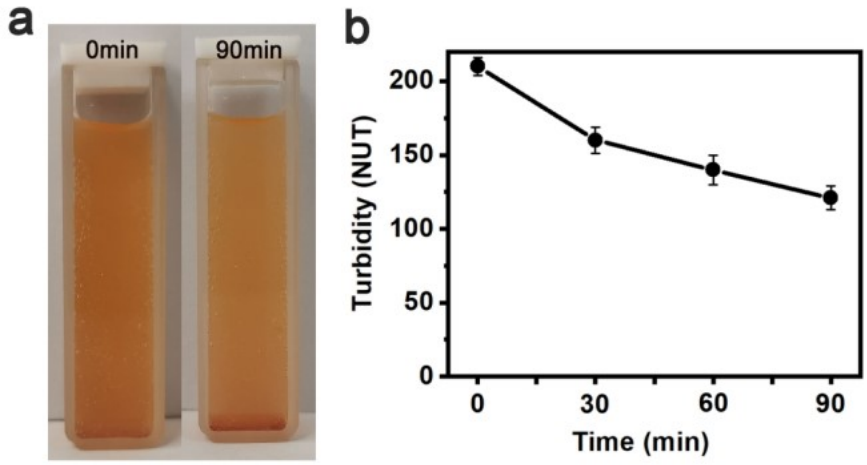


**Fig. S5.** (a) Photographs of VPNS dispersions after standing for 0 and 90 min. (b) Turbidity of VPNS dispersion as a function of aging time.

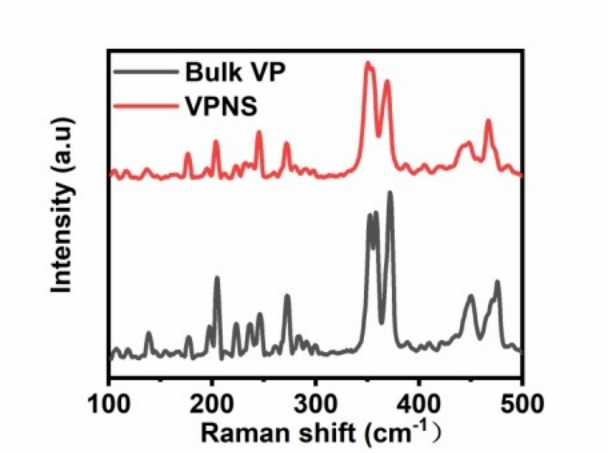


**Fig. S6.** Raman spectra of bulk VP and VPNS.

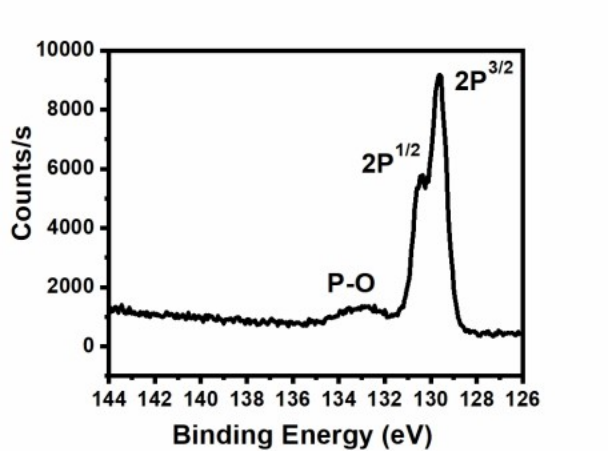


**Fig. S7.** XPS spectra of bulk VP. Three peaks located at about 129.7, 130.4, and 133.7 eV correspond to $2P_{3/2}$, $2P_{1/2}$, and $PO_x$.

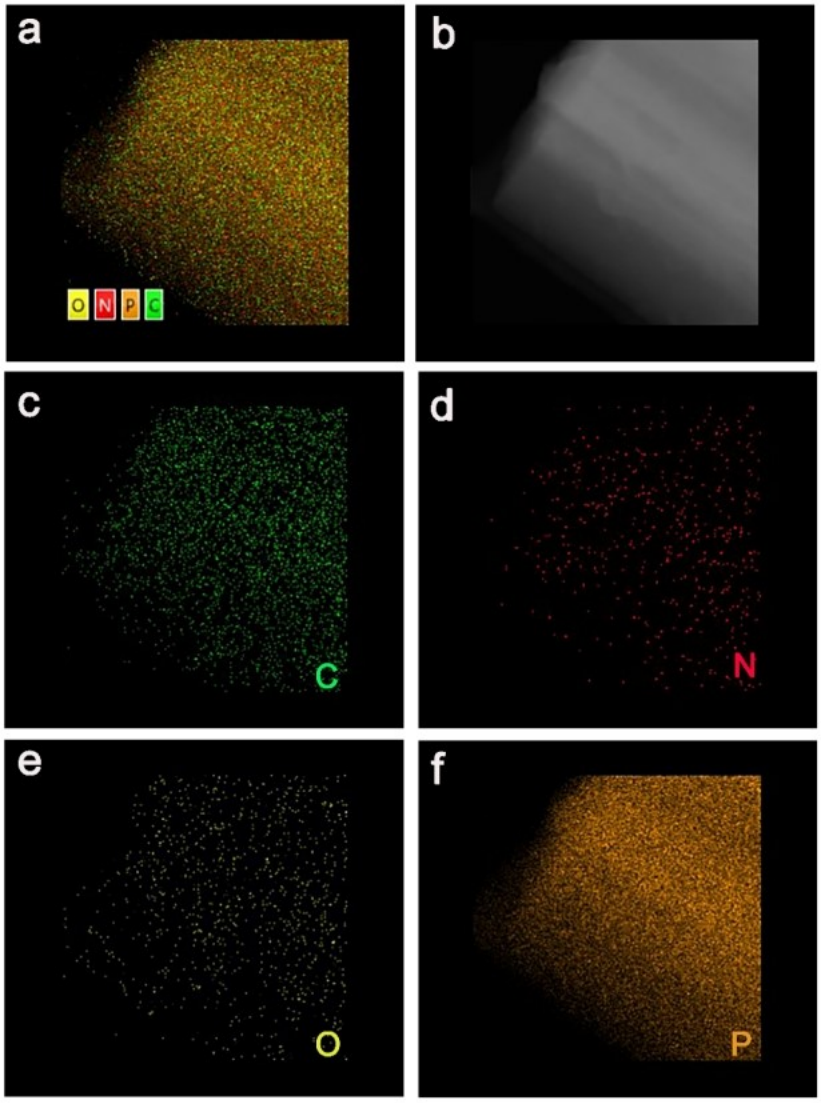


**Fig. S8.** Representative STEM mapping of VPNS.

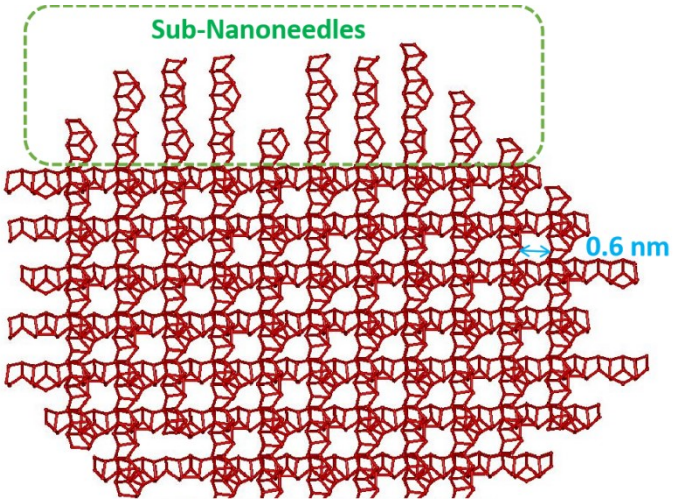


**Fig. S9.** Structural model of the monolayer violet phosphorene.

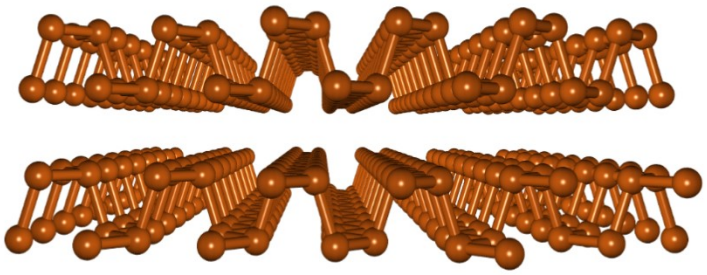

**Fig. S10.** Chemical structure of BPNS.

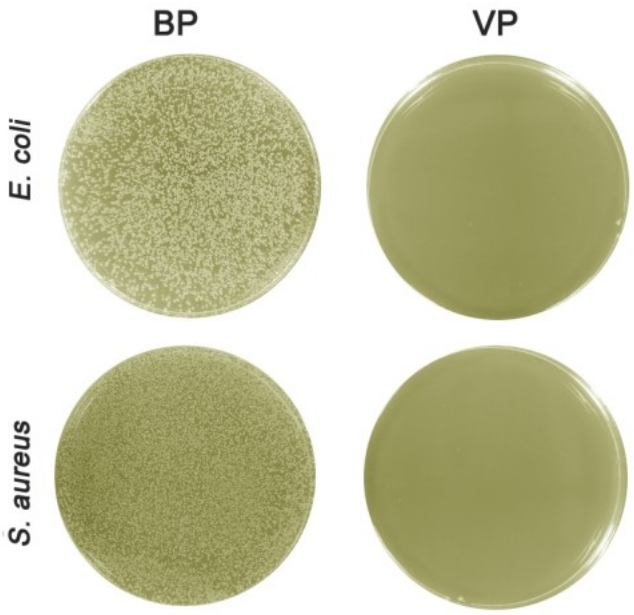


**Fig. S11.** Comparison of VP and BP antibacterial properties. Digital images of $10^7$ CFU·mL$^{-1}$ *E. coli* and *S.aureus* on agar-LB plates after exposure to 1.0 mg·mL$^{-1}$ bulk VP and BP under LED white light for 3 h.

.

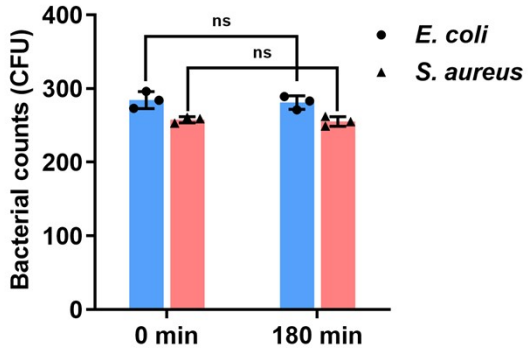


**Fig. S12.** The survival counts of bacteria under LED white light for 0 min and 180 min. Data are presented as the means ± SD (n = 3). *p < 0.05, **p < 0.01, ***p < 0.001, **** p<0.0001, ns, not significant.

a

| | MIC (mg mL$^{-1}$) | |
|---|---|---|
| | *E. coli* | *S. aureus* |
| VPNS | 0.8 | 0.8 |

b

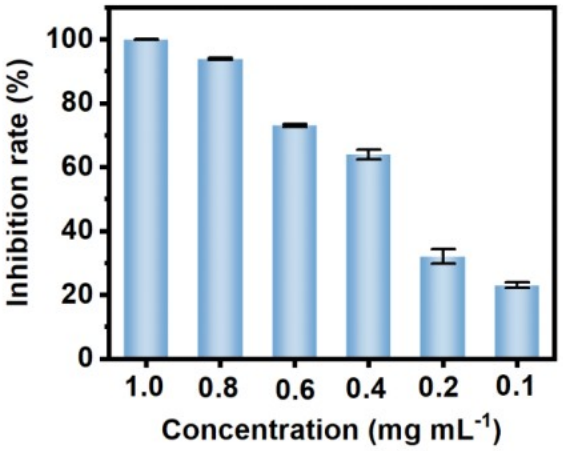


**Fig. S13.** (a) MIC and (b) MBC of VPNS on *E. coli* and *S. aureus.*

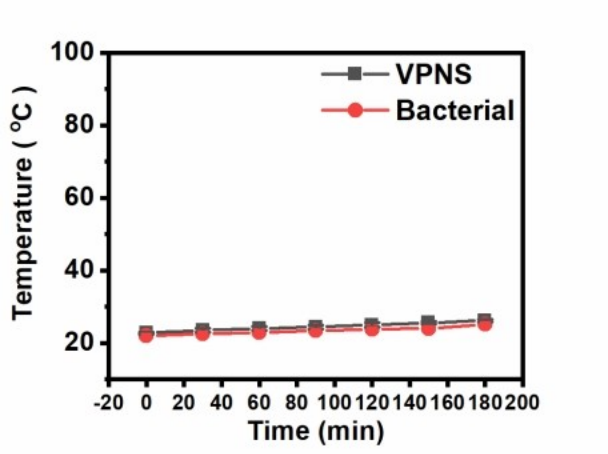


**Fig. S14.** Temperature change as a function of aging time in the presence of 1.0 mg·mL$^{-1}$ VPNS and bacteria under LED white light irradiation.

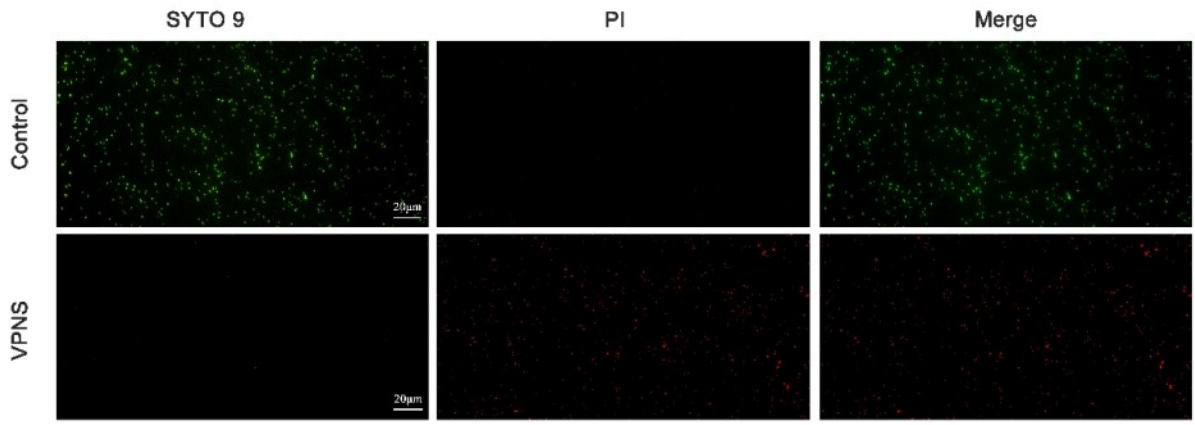


**Fig. S15.** Live/dead staining of *S. aureus* bacterial strains treated with VPNS under LED white light for 3 h (Live cells and dead cells are green and red, respectively).

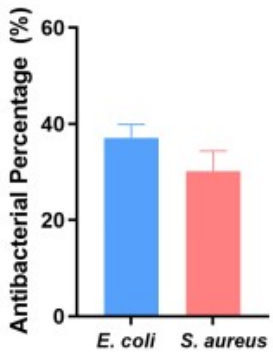


**Fig. S16.** Antibacterial percentage of the *E. coli* and *S. aureus* after exposure to 1.0 mg $mL^{-1}$ of VPNS for 3 h under dark conditions.

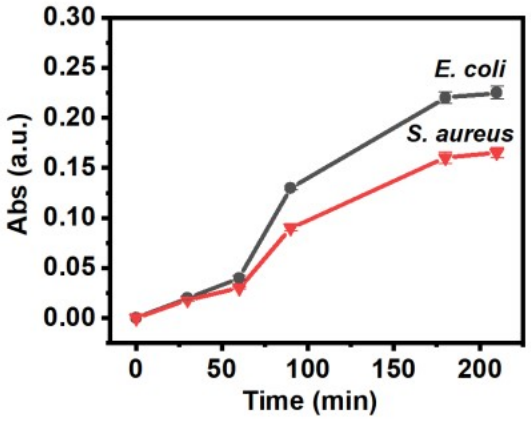


**Fig. S17.** DNA leakage kinetics of bacteria treated with VPNS under LED white light for 3 h.

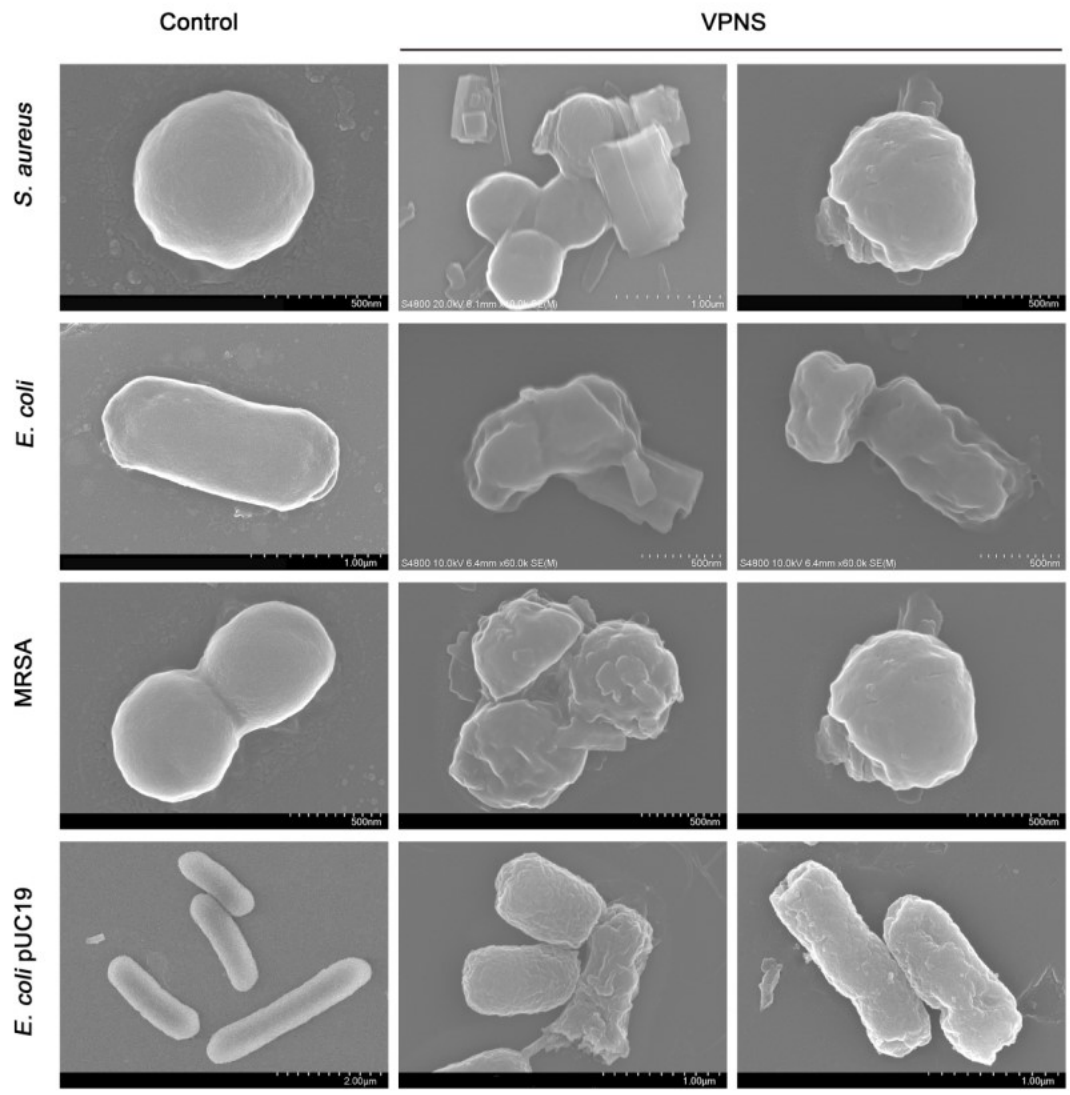


**Fig. S18.** SEM images showing morphological changes in *E. coli*, *S. aureus*, MRSA, and *E. coli* pUC19 before (controls) and after treatment with VPNS samples under LED white light for 3 h.

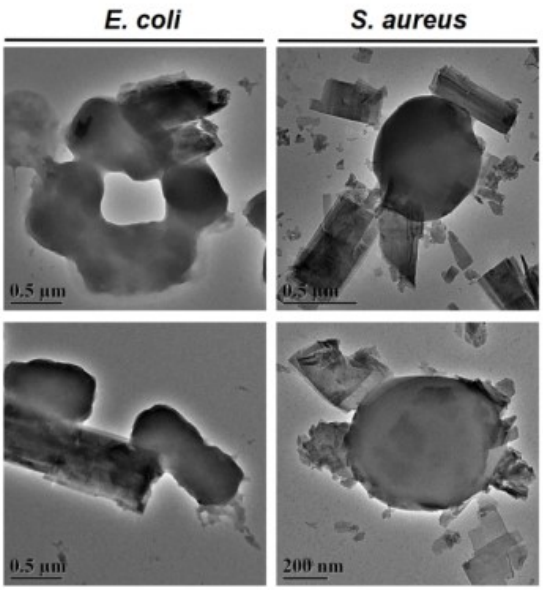


**Fig. S19**. TEM images showing morphological in *E. coli* and *S. aureus* after treatment with VPNS samples under dark conditions for 3 h.

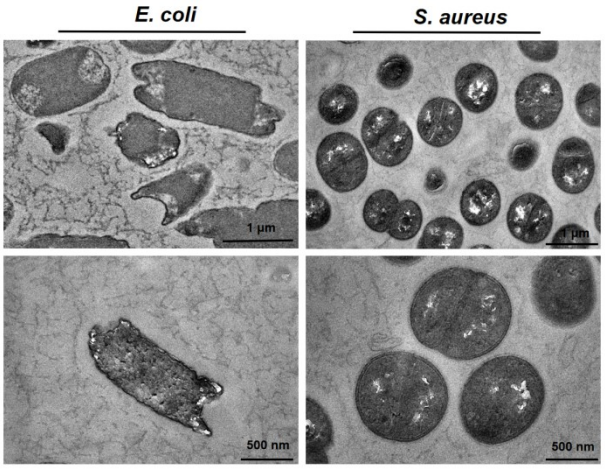


**Fig. S20.** TEM image of bacterial section showing morphological in E. coli and S. aureus after treatment with VPNS samples under dark conditions for 3 h.

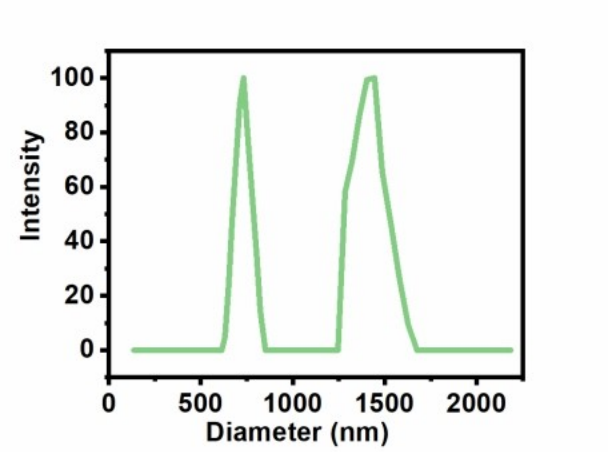


**Fig. S21.** DLS results for VPNS.

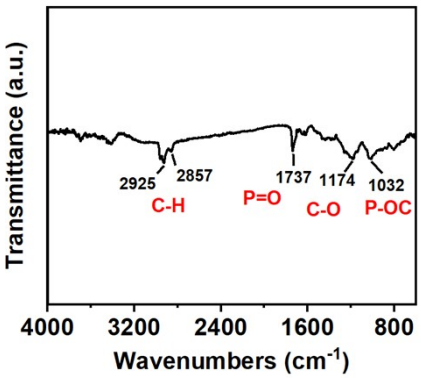


**Fig. S22.** FTIR spectrum of VPNS prepared by solvent exfoliation method.

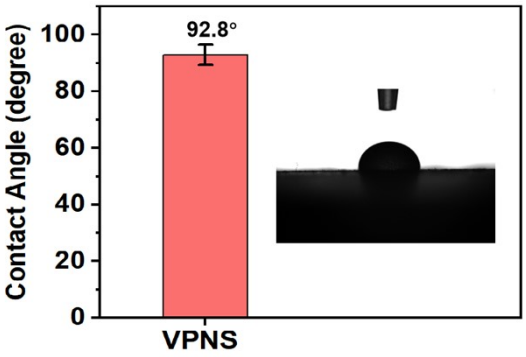


**Fig. S23**. Contact Angle between VPNS and water.

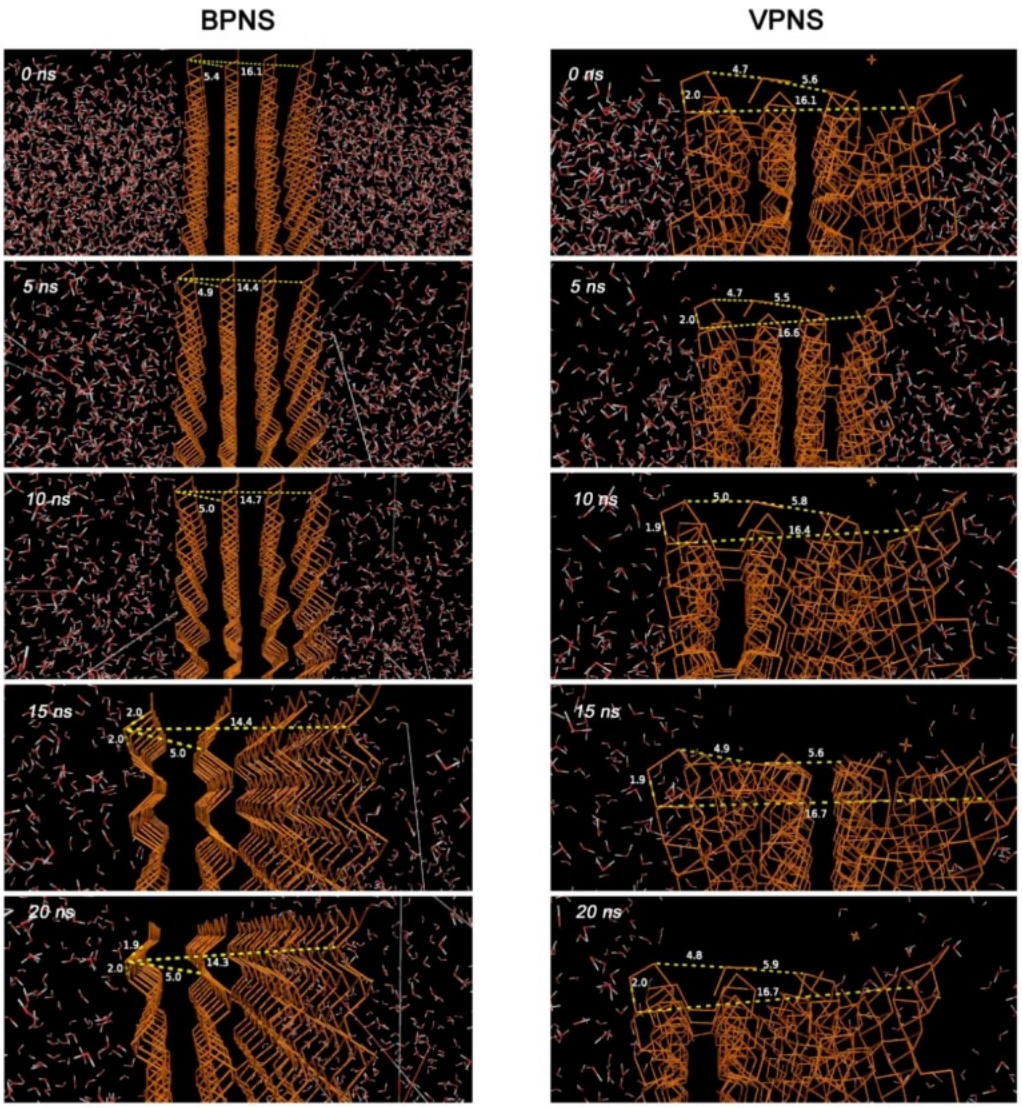


**Fig. S24.** BPNS and VPNS during NPT molecular dynamic simulation (0–20 ns).


**Fig. S25.** Inhibition zones of VPNS, BPNS, and $AgNO_3$ against *E. coli*.

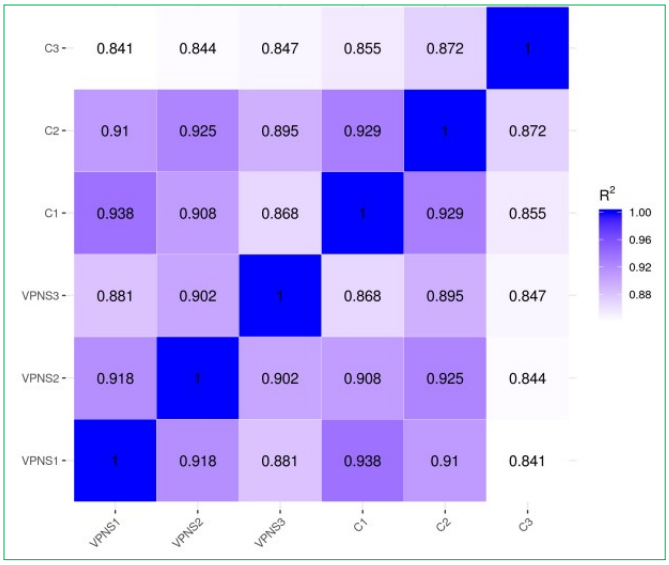


**Fig. S26.** Gene expression correlation map.

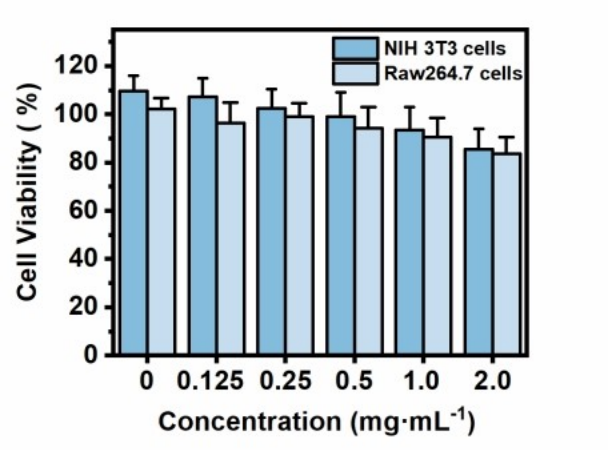


**Fig. S27.** Cytotoxicity of VPNS toward NIH 3T3 cells and Raw 264.7 cells within the concentration range of 0.125–2.0 mg·mL$^{-1}$.

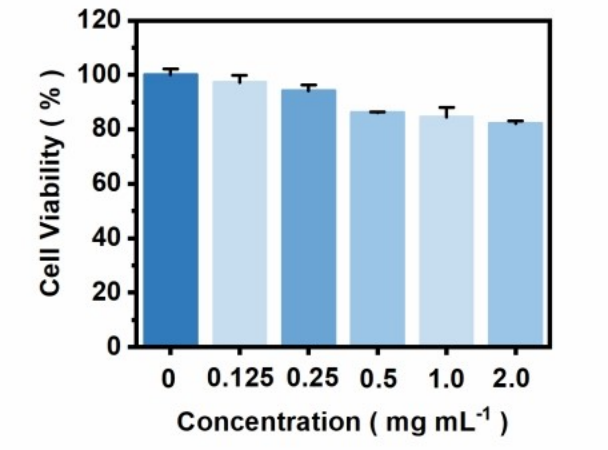


**Fig. S28**. Cell viability of L02 cells treated with VPNS in the concentration range of 0.125–2.0 mg·mL$^{-1}$ for 48 h.

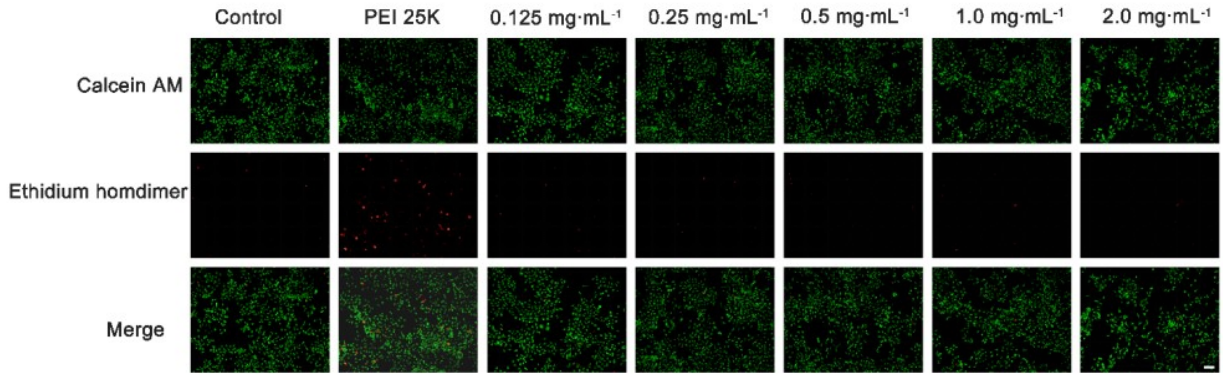


**Fig. S29.** Live/dead staining of L02 cells treated with different concentrations of VPNS.

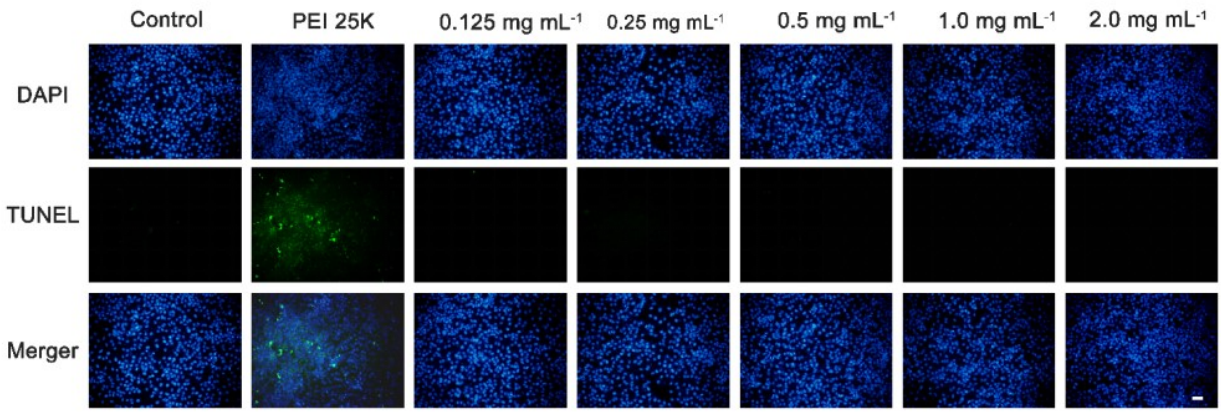


**Fig. S30.** TUNEL staining of L02 cells treated with different concentrations of VPNS.

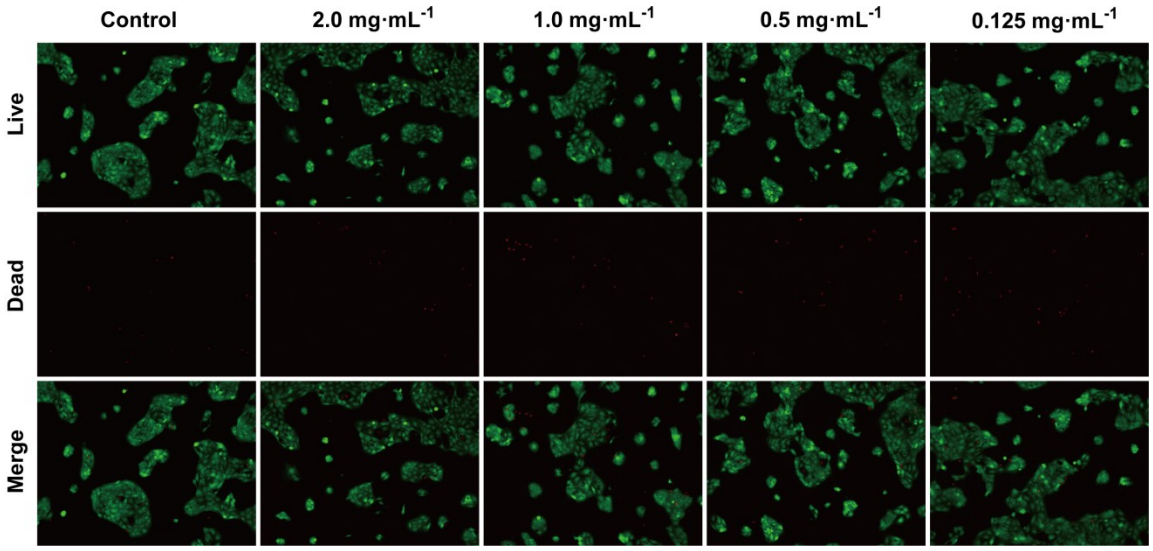


**Fig. S31.** Live/dead staining of HCEC cells treated with different concentrations of VPNS.

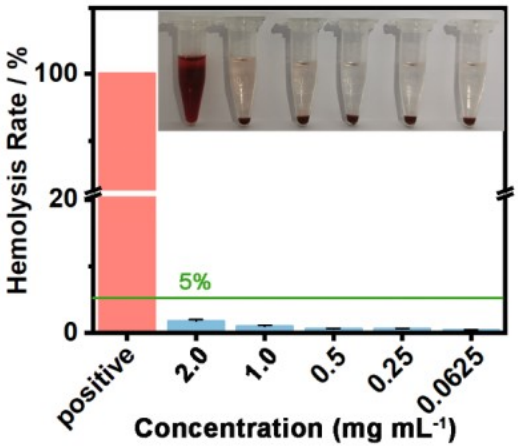


**Fig. S32.** Hemolysis rate of VPNS, and corresponding digital photos.

**Table S1.** Comparison of the antibacterial action of some typical nanomaterials

| Classification | Typical examples | Antibacterial action | Bacteria species | Experimental conditions | Antibacterial efficiency | Ref. |
|---|---|---|---|---|---|---|
| Phosphorus | VP | Sub-nanoneedles physical damage;<br>ROS-dependent oxidative stress | *E. coli*<br>*S. aureus*<br>MRSA<br>*E. coli*pUC19 | $10^7$ CFU/mL<br>LED light irradiation (3 h)<br>1.0 mg/mL | 99.99% | This work |
| | RP | Photocatalytic disinfection | *E. coli*<br>*S. aureus* | $10^6$ CFU/mL<br>20 min<br>400 μg/mL | 99.7% | 1–4 |
| | BP | ROS-dependent oxidative stress;<br>physical damage | *E. coli*<br>*B. subtilis*<br>*S. aureus* | 1. $10^7$ CFU/mL<br>LED light irradiation (3 h)<br>1.0 mg/mL<br>2. $10^8$ CFU/mL<br>12h<br>100 μg/mL | 99.99%<br>95% | 5–14 |
| Carbon | GO<br>RGO<br>GDY<br>GDYO | Nanoknives derived from the action of sharp edges | *E. coli*<br>*S. aureus*<br>*B. subtilis*<br>*S. mutans*<br>*F. nucleatum*<br>*P. gingivalis*<br>*P. syringae*<br>*F.* | | | 15–27 |

| | | | | | | |
|---|---|---|---|---|---|---|
| | | | *oxysporum*<br>*M. smegmatis* | 1. $10^5$ CFU/mL<br>LED light irradiation (90 min) | >99% | |
| | | ROS-dependent oxidative stress | *P. aeruginosa*<br>*E. coli*<br>*S. aureus*<br>MRSA | 3.0 mg/mL<br>2. $10^7$ CFU/mL<br>4 h | >99% | 28–34 |
| | | ROS-independent oxidative stress | *E. coli*<br>*S. aureus* | 200 μg/mL<br>3. $10^7$ CFU/mL | | 35–37 |
| | | Wrapping or trapping of bacterial membranes | *C. metalliduran s*<br>*E. coli*<br>*B. subtilis*<br>*R. opacus*<br>*P. syringae*<br>MRSA | 2 h<br>500 μg/mL | >90% | 38–43 |
| | | Other mechanisms | *E. coli* | | | 44–46 |
| TMDs | $MOS_2$<br>$WS_2$<br>$MOSe_2$ | ROS-dependent oxidative stress;<br>physical damage | MRSA<br>*P. aeruginosa*<br>*E. coli*<br>*B. subtilis* | $10^6$ CFU/mL<br>2 h<br>80 μg/mL | >90% | 47–54 |
| MXene | $Ti_3C_2Tx$ | ROS-dependent oxidative stress;<br>physical | *B. subtilis*<br>*E. coli*<br>*S. aureus* | $10^7$ CFU/mL<br>4 h<br>100 μg/mL | 97.70% | 55–63 |

| | | | | | |
|---|---|---|---|---|---|
| | damage | MRSA<br>VRE | | | |
| g-$C_3N_4$ | Photocatalytic disinfection | *E. coli*<br>*S. aureus*<br>*E. faecalis*<br>*S. typhimurium* | 1. $10^6$ CFU/mL<br>Visible light irradiation (12 h)<br>200 μg/mL | >99% | 64–74 |
| | | | 2. $10^6$ CFU/mL<br>Visible light irradiation (3 h)<br>60 μg/mL | <10% | |

**References**


[1] D. Xia, Z. Shen, G. Huang, W. Wang, J. C. Yu, P. K. Wong, *Environ. Sci. Technol.* **2015**, *49*, 6264-6273.

[2] J. Li, X. Liu, L. Tan, Y. Liang, Z. Cui, X. Yang, S. Zhu, Z. Li, Y. Zheng, K. W. K. Yeung, X. Wang, S. Wu, *Small Methods* **2019**, *3*, 1900048.

[3] J. Liu, Y. Zhu, J. Chen, D. S. Butenko, J. Ren, X. Yang, P. Lu, P. Meng, Y. Xu, D. Yang, S. Zhang, *J. Hazard. Mater.* **2021**, *413*, 125462.

[4] W. Wang, G. Li, T. An, D. K. L. Chan, J. C. Yu, P. K. Wong, *Appl. Catal B- Environ.* **2018**, *238*, 126-135.

[5] M. Liang, M. Zhang, S. Yu, Q. Wu, K. Ma, Y. Chen, X. Liu, C. Li, F. Wang, *Small* **2020**, *16*, e1905938.

[6] H. Wang, S. Jiang, W. Shao, X. Zhang, S. Chen, X. Sun, Q. Zhang, Y. Luo, Y. Xie, *J. Am. Chem. Soc.* **2018**, *140*, 3474-3480.

[7] H. Wang, X. Yang, W. Shao, S. Chen, J. Xie, X. Zhang, J. Wang, Y. Xie, *J. Am. Chem. Soc.* **2015**, *137*, 11376-11382.

[8] Z. Xiong, X. Zhang, S. Zhang, L. Lei, W. Ma, D. Li, W. Wang, Q. Zhao, B. Xing, *Ecotoxicol. Environ. Saf.* **2018**, 161, 507-514.

[9] D. Zhang, H. M. Liu, X. Shu, J. Feng, P. Yang, P. Dong, X. Xie, Q. Shi, *J. Hazard. Mater.* **2020**, *393*, 122317.

[10] W. Liu, Y. Zhang, Y. Zhang, A. Dong, *Chem. Eur. J.* **2020**, *26*, 2478-2485.

[11] D. A. Reddy, E. H. Kim, M. Gopannagari, Y. Kim, D. P. Kumar, T. K. Kim, *Appl. Catal B-Environ.* **2019**, 241, 491-498.

[12] L. Tan, J. Li, X. Liu, Z. Cui, X. Yang, K. W. K. Yeung, H. Pan, Y. Zheng, X. Wang, S. Wu, *Small* **2018**, *14*,1703197.

[13] H. Wang, X. F. Yu, *Small* **2018**, *14*,1702830.

[14] Z. Yuan, J. Li, M. Yang, Z. Fang, J. Jian, D. Yu, X. Chen, L. Dai, *J. Am. Chem. Soc.* **2019**, *141*, 4972-4979.

[15] O. Akhavan, E. Ghaderi, *ACS Nano* **2010**, *4*, 5731-5736.

[16] J. Chen, X. Wang, H. Han, *J. Nanopart. Res.* **2013**, *15*,1-14.

[17] A. V. Titov, P. Král, R. Pearson, *ACS Nano* **2010**, *1*, 229-34.

[18] F. Perreault, A. F. d. Faria, S. Nejati, M. Elimelech, *ACS Nano* **2015**, *9*,7226-36.

[19] W. Hu, C. Peng, W. Luo, M. Lv, X. Li, Q. Huang, C. Fan, *ACS Nano.* **2010**, *4*, 4317-4323.

[20] J. Chen, H. Peng, X. Wang, F. Shao, Z. Yuan, H. Han, *Nanoscale* **2014**, *6*, 1879-1889.

[21] R. Guo, J. Mao, L. T. Yan, *Biomaterials* **2013**, *34*, 4296-4301.

[22] J. He, X. Zhu, Z. Qi, C. Wang, X. Mao, C. Zhu, Z. He, M. Li, Z. Tang, *ACS Appl. Mater. Interfaces* **2015**, *7*, 5605-5611.

[23] Y. Li, H. Yuan, A. von dem Bussche, M. Creighton, R. H. Hurt, A. B. Kane, H. Gao, *Proc. Natl. Acad. Sci. USA*. **2013**, *110*, 12295-12300.

[24] J. D. Mangadlao, C. M. Santos, M. J. Felipe, A. C. de Leon, D. F. Rodrigues, R. C. Advincula, *Chem. Commun*. **2015**, *51*, 2886-2889.

[25] Y. L. F. Musico, C. M. Santos, M. L. P. Dalida, D. F. Rodrigues, *ACS Sustainable Chem. Eng.* **2014**, *2*, 1559-1565.

[26] J. Wang, Y. Wei, X. Shi, H. Gao, *RSC Adv.* **2013**, *3*, 15776.

[27] F. Zou, H. Zhou, D. Y. Jeong, J. Kwon, S. U. Eom, T. J. Park, S. W. Hong, J. Lee, *ACS Appl. Mater. Interfaces* **2017**, *9*, 1343-1351.

[28] Y. Chong, C. Ge, G. Fang, X. Tian, X. Ma, T. Wen, W. G. Wamer, C. Chen, Z. Chai, J. J. Yin, *ACS Nano* **2016**, *10*, 8690-8699.

[29] Y. Chong, C. Ge, G. Fang, R. Wu, H. Zhang, Z. Chai, C. Chen, J. J. Yin, *Environ. Sci. Technol.* **2017**, *51*, 10154-10161.

[30] Y. Feng, Q. Chen, Q. Yin, G. Pan, Z. Tu, L. Liu, *ACS Appl. Bio Mater*. **2019**, *2*, 747−756.

[31] S. Gurunathan, J. W. Han, A. A. Dayem, V. Eppakayala, J. H. Kim, *Int. J. Nanomed*. **2012**, *7*, 5901–5914.

[32] Y. Li, Y. Liu, Y. Fu, T. Wei, L. Le Guyader, G. Gao, R. S. Liu, Y. Z. Chang, C. Chen, *Biomaterials* **2012**, *33*, 402-411.

[33] L. Wang, Y. Li, Y. Wang, W. Kong, Q. Lu, X. Liu, D. Zhang, L. Qu, *ACS Appl. Mater. Interfaces* **2019**, *11*, 21822-21829.

[34] Y. Zhang, W. Liu, Y. Li, Y. W. Yang, A. Dong, Y. Li, *iScience* **2019**, *19*, 662-675.

[35] J. Li, G. Wang, H. Zhu, M. Zhang, X. Zheng, Z. Di, X. Liu, X. Wang, *Sci. Rep*. **2014**, *4*, 4359.

[36] S. Liu, T. Zeng, M. Hofmann, E. Burcombe, J. Wei, R. Jiang, J. Kong, Y. Chen, *ACS Nano* **2011**, *5*, 6971-6980.

[37] J. Chen, X. Wang, H. Han, *J. Nanopart. Res*. **2013**, *15*, 1-14.

[38] O. Akhavan, E. Ghaderi, A. Esfandiar, *J. Phys. Chem. B* **2011**, *115*, 6279–6288.

[39] M. Dallavalle, M. Calvaresi, A. Bottoni, M. Melle-Franco, F. Zerbetto, *ACS Appl. Mater. Interfaces* **2015**, *7*, 4406-4414.

[40 R. Kanchanapally, B. P. Viraka Nellore, S. S. Sinha, F. Pedraza, S. J. Jones, A. Pramanik, S. R. Chavva, C. Tchounwou, Y. Shi, A. Vangara, D. Sardar, P. C. Ray, *RSC. Adv*. **2015**, *5*, 18881-18887.

[41] S. Liu, M. Hu, T. H. Zeng, R. Wu, R. Jiang, J. Wei, L. Wang, J. Kong, Y. Chen, *Langmuir* **2012**, *28*, 12364-12372.

[42] I. E. Mejias Carpio, C. M. Santos, X. Wei, D. F. Rodrigues, *Nanoscale* **2012**, *4*, 4746-4756.

[43] K. H. Tan, S. Sattari, I. S. Donskyi, J. L. Cuellar-Camacho, C. Cheng, K. Schwibbert, A. Lippitz, W. E. S. Unger, A. Gorbushina, M. Adeli, R. Haag, *Nanoscale* **2018**, *10*, 9525-9537.

[44] O. Akhavan, E. Ghaderi, *Carbon* **2012**, *50*, 1853-1860;

[45] Y. Tu, M. Lv, P. Xiu, T. Huynh, M. Zhang, M. Castelli, Z. Liu, Q. Huang, C. Fan, H. Fang, R. Zhou, *Nat. Nanotechnol*. **2013**, *8*, 594-601.

[46] B. Q. Luan, T. Huynh, L. Zhao, R. H. Zhou, *ACS Nano* **2015**, *9*, 663-669.

[47] J. Fan, Y. Li, H. N. Nguyen, Y. Yao, D. F. Rodrigues, *Environ Sci-Nano*. **2015**, *2*, 370-379.

[48] D. K. Ji, Y. Zhang, Y. Zang, J. Li, G. R. Chen, X. P. He, H. Tian, *Adv. Mater.* **2016**, *28*, 9356-9363.

[49] S. Karunakaran, S. Pandit, B. Basu, M. De, *J. Am. Chem. Soc.* **2018**, *140*, 12634-12644.

[50] T. I. Kim, J. Kim, I. J. Park, K. O. Cho, S. Y. Choi, *2D Mater.* **2019**, *6*, 025025.

[51] C. Liu, D. Kong, P. C. Hsu, H. Yuan, H. W. Lee, Y. Liu, H. Wang, S. Wang, K. Yan, D. Lin, P. A. Maraccini, K. M. Parker, A. B. Boehm, Y. Cui, *Nat. Nanotechnol.* **2016**, *11*, 1098-1104.

[52] S. Pandit, S. Karunakaran, S. K. Boda, B. Basu, M. De, *ACS Appl. Mater. Interfaces* **2016**, *8*, 31567-31573.

[53] W. Yin, J. Yu, F. Lv, L. Yan, L. R. Zheng, Z. Gu, Y. Zhao, *ACS Nano* **2016**, *10*, 11000-11011.

[54] D. Kong, H. Wang, J. J. Cha, M. Pasta, K. J. Koski, J. Yao, Y. Cui, *Nano Lett.* **2013**, *13*,1341-1347.

[55] R. P. Pandey, P. A. Rasheed, T. Gomez, K. Rasool, J. Ponraj, K. Prenger, M. Naguib, K. A. Mahmoud, *ACS Appl. Nano Mater*. **2020**, *3*, 11372-11382.

[56] K. Rajavel, S. Shen, T. Ke, D. Lin, *2D Mater*. **2019**, *6*, 035040.

[57] K. Rasool, M. Helal, A. Ali, C. E. Ren, Y. Gogotsi, K. A. Mahmoud, *ACS Nano* **2016**, *10*, 3674-3684.

[58] K. Zheng, S. Li, L. Jing, P. Y. Chen, J. Xie, *Adv. Healthc. Mater*. **2020**, *9*, 2001007.

[59] F. Alimohammadi, M. Sharifian Gh, N. H. Attanayake, A. C. Thenuwara, Y. Gogotsi, B. Anasori, D. R. Strongin, *Langmuir* **2018**, *34*, 7192-7200.

[60] A. Arabi Shamsabadi, M. Sharifian Gh, B. Anasori, M. Soroush, *ACS Sustainable Chem. Eng.* **2018**, *6*, 16586-16596.

[61] A. M. Jastrzębska, E. Karwowska, T. Wojciechowski, W. Ziemkowska, A. Rozmysłowska, L. Chlubny, A. Olszyna, *J. Mater. Eng. Perform*. **2018**, *28*, 1272-1277.

[62] K. Rasool, K. A. Mahmoud, D. J. Johnson, M. Helal, G. R. Berdiyorov, Y. Gogotsi, *Sci. Rep*. **2017**, *7*, 1598.

[63] F. Wu, H. Zheng, W. Wang, Q. Wu, Q. Zhang, J. Guo, B. Pu, X. Shi, J. Li, X. Chen, W. Hong, *Sci. China Mater*. **2020**, *64*, 748-758.

[64] W. Bing, Z. Chen, H. Sun, P. Shi, N. Gao, J. Ren, X. Qu, *Nano. Res*. **2015**, *8*, 1648-1658.

[65] N. He, S. Cao, L. Zhang, Z. Tian, H. Chen, F. Jiang, *Chemosphere* **2019**, *235*, 1116-1124.

[66] N. S. Heo, S. Shukla, S. Y. Oh, V. K. Bajpai, S. U. Lee, H. J. Cho, S. Kim, Y. Kim, H. J. Kim, S. Y. Lee, Y. S. Jun, M. H. Oh, Y. K. Han, S. M. Yoo, Y. S. Huh, *Mater. Sci. Eng. C-Mater*. **2019**, *104*, 109846.

[67] R. Li, Y. Ren, P. Zhao, J. Wang, J. Liu, Y. Zhang, *J. Hazard. Mater*. **2019**, *365*, 606-614.

[68] Y. Li, C. Zhang, D. Shuai, S. Naraginti, D. Wang, W. Zhang, *Water Res*. **2016**, *106*, 249-258.

[69] V. Shanmugam, A. L. Muppudathi, S. Jayavel, K. S. Jeyaperumal, *Arab. J. Chem*. **2020**, *13*, 2439–2455.

[70] Z. Wang, K. Dong, Z. Liu, Y. Zhang, Z. Chen, H. Sun, J. Ren, X. Qu, *Biomaterials* **2017**, *113*, 145-157.

[71] B. Wu, Y. Li, K. Su, L. Tan, X. Liu, Z. Cui, X. Yang, Y. Liang, Z. Li, S. Zhu, K. W. K. Yeung, S. Wu, *J. Hazard. Mater*. **2019**, *377*, 227-236.

[72] J. Xu, Z. Wang, Y. Zhu, *ACS Appl. Mater. Interfaces* **2017**, *9*, 27727-27735.

[73] K. Yan, C. Mu, L. Meng, Z. Fei, P. J. Dyson, *Nanoscale Adv*. **2021**, *3*, 3708-3729.

[74] X. Zeng, Y. Liu, Y. Xia, M. H. Uddin, D. Xia, D. T. McCarthy, A. Deletic, J. Yu, X. Zhang, *Appl Catal. B-Environ*. **2020,** *274*, 119095.